Computational Journal of Mathematical and Statistical Sciences
4(2), 476–499
DOI:10.21608/cjmss.2025.374786.1155
https://cjmss.journals.ekb.eg/

Research article

Advancing Lifetime Data Modeling via the Marshall-Olkin Cosine Topp-Leone Distribution Family

Abdulhameed Ado Osi[1,*], **Gaber Sallam Salem Abdalla**[2], **Narinderjit Singh Sawaran Singh**[3], **Ahmad Abubakar Suleiman**[4]

[1] Department of Statistics, Aliko Dangote University of Science and Technology, Wudil 713101, Nigeria.

[2] Department of Insurance and Risk Management, Faculty of Business, Imam Mohammad Ibn Saud Islamic University (IMSIU), Riyadh 11432, Saudi Arabia; jssabdullah@imamu.edu.sa.

[3] Faculty of Data Science and Information Technology, INTI International University, Persiaran Perdana BBN Putra Nilai 71800, Malaysia; Narinderjits.sawaran@newinti.edu.my.

[4] Department of Statistics, Aliko Dangote University of Science and Technology, Wudil 713101, Nigeria; ahmadabubakar31@gmail.com.

* **Correspondence:** aaosiwudil@kustwudil.edu.ng

Abstract: Probability distributions are fundamental tools in statistical modeling, particularly in the analysis of lifetime, reliability, and epidemiological data. Classical distributions such as the exponential, Weibull, and gamma, while analytically convenient, often lack the flexibility required to model complex real-world phenomena, such as skewness, heavy tails, and intricate dependence structures. In response to these limitations, this paper introduces a novel trigonometric-based extension of the Marshall-Olkin family, termed the Marshall-Olkin Cosine Topp-Leone (MOCTL) distribution family. This new family incorporates additional shape parameters that allow for greater modeling flexibility and adaptability across various data types. We derive and explore several important statistical properties of the proposed family, including its density, distribution, hazard rate, and quantile functions. Parameter estimation is addressed using the maximum likelihood estimation (MLE) method, and a detailed Monte Carlo simulation is conducted to assess the performance, bias, and consistency of the MLEs. The real-world applicability of the MOCTL family is demonstrated through three datasets, including medical and epidemiological studies. Furthermore, a log-MOCTL Weibull regression model is proposed and applied to HIV/TB and COVID-19 datasets, confirming its superior modeling capability.

Keywords: Marsharl-Olkin family, Cosine G family, Simulation study, Maximum likelihood estimation, Survival Regression Model, Cox-Snail residual Analysis.
Mathematics Subject Classification: 62E15, 62G08.
Received: 14 April 2025; Revised: 15 June 2025; Accepted: 17 June 2025; Online: 19 June 2025.

1. Introduction

In many real-world applications, standard probability distributions often fall short in adequately modeling complex data structures [1]. As a result, there has been a growing interest in extending classical models by incorporating additional parameters to increase their flexibility [2]. Over the past two decades, numerous generalized distribution families have been developed and successfully applied across diverse domains such as biology, engineering, economics, environmental science, medicine, and finance.

Prominent among these generalizations is the exponentiated-G family proposed by [3], which introduces a shape parameter into the cumulative distribution function (CDF). Other notable contributions include the Marshall-Olkin family [4], the beta-G family [5], the quadratic transmutation family [6], the odd generalized NH-G family [7], the Topp–Leone modified Weibull model [8], the Kumaraswamy-G family [9], and the gamma-G family [10]. Additional developments include the logistic-X family by [11] and the T-X family explored by [12].

The Marshall-Olkin (MO) family, first introduced by [4], has gained significant attention for its versatility in statistical modeling. [13] offered a comprehensive analysis of its mathematical properties and introduced several new distributions under the MO framework. Subsequent extensions have aimed to further enhance its applicability. For example, [14] proposed the MO alpha power family, enabling broader data modeling capabilities. Ref. [15] examined the MO discrete uniform distribution, analyzing its hazard rate and entropy, while [16] developed the MO generalized-G family with a focus on theoretical and applied implications. Similarly, [17] introduced the Topp-Leone MO-G family, effectively capturing heavy-tailed data and varying hazard functions. Applications of the MO framework include the MO exponentiated Dagum distribution in empirical studies [18], and the MO odd power generalized Weibull distribution for modeling COVID-19 data [19]. Furthermore, the MO Type II Topp-Leone-G family has demonstrated power-law behavior common in real-world datasets [20]. Recent contributions include the MO generalized-k family [21], the exponentiated half-logistic generalized MO-G family [22], cosine Fréchet loss distribution [23], and the MO Lomax distribution [24]. More recently, [25] proposed the cosine MO-G family, which incorporates trigonometric transformation into the MO framework, demonstrating promising results in tail modeling.

In parallel, the trigonometric-G family of distributions, which employs trigonometric transformations to induce flexibility, has also seen growing interest. Key contributions in this area include the sine TL-G (STLG) family by [26], the sine Kumaraswamy-G family [27], the alpha-sine-G family [28], and the sine exponential distribution [29]. Additional developments include the tan-G family by [30], the cosine Topp-Leone-G (CTL-G) families proposed by [31], estimation of arctan uniform distribution using ranked set sampling studied by [32], the sine generalized linear exponential model discussed by [33], truncated inverted arctan power distribution proposed by [34], sine-exponentiated Weibull-G family investigated by [35], new extended cosine-G distributions studied by [36], statistical inference under censored data for the new exponential-X Fréchet distribution proposed by [37], sine inverse exponential model investigated by [38] and the cosine-geometric distribution introduced by [39]. These trigonometric-based models significantly expand the toolkit for modeling diverse data behaviors.

While recent models such as the CTL-G [31] and TrCTL-G [40] families have proven effective, they may still be limited in controlling tail behavior and asymmetry. To address these limitations, we propose a novel distributional family-the Marshall-Olkin Cosine Topp-Leone G (MOCTL-G) family-by integrating the Marshall-Olkin mechanism into the CTL-G generator. The Marshall-Olkin transformation contributes an additional parameter that directly affects the distribution's tail behavior and failure rate, offering enhanced flexibility for datasets exhibiting skewness, kurtosis, or heavy tails.

Therefore, the novelty of our contribution lies in the trigonometric extension of the Marshall-Olkin framework via the cosine Topp-Leone generator, resulting in a new and highly adaptable family of distributions. This development enriches the existing literature by offering a powerful tool for modeling complex lifetime, reliability, and epidemiological data.

2. The proposed Family

Here, we introduce the MOCTL-G family and outline its key mathematical properties. This family is constructed by incorporating the Marshall-Olkin transformation into the Cosine Topp-Leone G (CTLG) family [31]. The cumulative distribution function (CDF) of the CTLG distribution is defined as:

$$F(t;\eta,\psi) = 1 - \cos\left[\frac{\pi}{2}\left(1 - \bar{H}(t;\psi)^2\right)^{\eta}\right], \quad t \in \Re,\ \eta > 0, \tag{2.1}$$

where $\bar{H}(t;\psi) = 1 - H(t;\psi)$ represents the survival function of the baseline distribution.

The probability density function (PDF) corresponding to this distribution is given as:

$$f(t;\eta,\psi) = \pi\eta H(t;\psi)\bar{H}(t;\psi)\left(1 - \bar{H}(t;\psi)^2\right)^{\eta-1}\sin\left[\frac{\pi}{2}\left(1 - \bar{H}(t;\psi)^2\right)^{\eta}\right]. \tag{2.2}$$

To extend this model, we apply the Marshall-Olkin transformation [4], which modifies a given baseline CDF $H(w)$ to create a more flexible family:

$$F(w;\vartheta,\psi) = \frac{H(w)}{\vartheta + (1-\vartheta)H(w)}, \tag{2.3}$$

where $0 < \vartheta < 1$ is an additional shape parameter that enhances flexibility. The corresponding PDF is:

$$f(w;\vartheta,\psi) = \frac{\vartheta h(w)}{[\vartheta + (1-\vartheta)H(w)]^2}. \tag{2.4}$$

Let T be a random variable following the MOCTL-G family with parameters η, ϑ, and the baseline parameter vector ψ. Then, the CDF and PDF are given as:

$$F_{MOCTL-G}(t;\eta,\vartheta,\psi) = \frac{1 - \cos\left[\frac{\pi}{2}\left(1 - \bar{H}(t;\psi)^2\right)^{\eta}\right]}{1 - \vartheta\cos\left[\frac{\pi}{2}\left(1 - \bar{H}(t;\psi)^2\right)^{\eta}\right]}, \tag{2.5}$$

and

$$f_{MOCTL-G}(t;\eta,\vartheta,\psi) = \frac{\pi\eta\vartheta H(t;\psi)\bar{H}(t;\psi)\left(1 - \bar{H}(t;\psi)^2\right)^{\eta-1}\sin\left[\frac{\pi}{2}\left(1 - \bar{H}(t;\psi)^2\right)^{\eta}\right]}{[1 - \vartheta\cos\left(\frac{\pi}{2}\left(1 - \bar{H}(t;\psi)^2\right)^{\eta}\right)]^2}, \tag{2.6}$$

where $\bar{H}(t;\psi) = 1 - H(t;\psi)$.

Proof. The Marshall-Olkin transformation modifies a given baseline CDF $M(x)$, as seen in Eq. (5). Applying this transformation to the CTLG distribution leads to:

$$F_{MOCTL-G}(t;\eta,\vartheta,\psi)=\frac{1-\cos\left[\frac{\pi}{2}\left(1-\bar{H}(t;\psi)^2\right)^{\eta}\right]}{1-\vartheta\cos\left[\frac{\pi}{2}\left(1-\bar{H}(t;\psi)^2\right)^{\eta}\right]}. \tag{2.7}$$

Taking the first derivative of Equation (2.7) with respect to t results in the PDF:

$$f_{MOCTL-G}(t;\eta,\vartheta,\psi)=\frac{\pi\eta\vartheta H(t;\psi)\bar{H}(t;\psi)\left(1-\bar{H}(t;\psi)^2\right)^{\eta-1}\sin\left[\frac{\pi}{2}\left(1-\bar{H}(t;\psi)^2\right)^{\eta}\right]}{[1-\vartheta\cos\left(\frac{\pi}{2}\left(1-\bar{H}(t;\psi)^2\right)^{\eta}\right)]^2}. \tag{2.8}$$

Thus, the proof is complete. □ □

2.1. Reliability Functions of MOCTL-G

This part provides various reliability measures for the MOCTL-G family, including the survival function (SF), hazard rate function (HRF), reverse hazard function (RHF), odd function, and cumulative hazard function (CHF).

The SF of MOCTL-G family is given by:

$$S(t;\eta,\vartheta,\psi)=1-\frac{1-\cos\left[\frac{\pi}{2}\left(1-\bar{H}(t;\psi)^2\right)^{\eta}\right]}{1-\vartheta\cos\left[\frac{\pi}{2}\left(1-\bar{H}(t;\psi)^2\right)^{\eta}\right]}. \tag{2.9}$$

The HRF of MOCTL-G family is defined as:

$$h(t;\eta,\vartheta,\psi)=\frac{\pi\eta\vartheta H(t;\psi)\bar{H}(t;\psi)\left(1-\bar{H}(t;\psi)^2\right)^{\eta-1}\sin\left[\frac{\pi}{2}\left(1-\bar{H}(t;\psi)^2\right)^{\eta}\right]}{\left[1-\vartheta\cos\left(\frac{\pi}{2}\left(1-\bar{H}(t;\psi)^2\right)^{\eta}\right)\right]^2\cdot S(x)}. \tag{2.10}$$

The RHF of MOCTL-G family is derive as:

$$r(t;\eta,\vartheta,\psi)=\frac{\pi\eta\vartheta H(t;\psi)\bar{H}(t;\psi)\left(1-\bar{H}(t;\psi)^2\right)^{\eta-1}\sin\left[\frac{\pi}{2}\left(1-\bar{H}(t;\psi)^2\right)^{\eta}\right]}{\left[1-\vartheta\cos\left(\frac{\pi}{2}\left(1-\bar{H}(t;\psi)^2\right)^{\eta}\right)\right]^2\left(1-\cos\left[\frac{\pi}{2}\left(1-\bar{H}(t;\psi)^2\right)^{\eta}\right]\right)}. \tag{2.11}$$

The odd function of MOCTL-G family is expressed as:

$$\Theta(t;\eta,\vartheta,\psi)=\frac{F(t;\eta,\vartheta,\psi)}{S(t;\eta,\vartheta,\psi)}=\frac{\frac{1-\cos\left[\frac{\pi}{2}\left(1-\bar{H}(t;\psi)^2\right)^{\eta}\right]}{1-\vartheta\cos\left[\frac{\pi}{2}\left(1-\bar{H}(t;\psi)^2\right)^{\eta}\right]}}{1-\frac{1-\cos\left[\frac{\pi}{2}\left(1-\bar{H}(t;\psi)^2\right)^{\eta}\right]}{1-\vartheta\cos\left[\frac{\pi}{2}\left(1-\bar{H}(t;\psi)^2\right)^{\eta}\right]}}. \tag{2.12}$$

Finally, the CHF of MOCTL-G family is given by:

$$H(t;\eta,\vartheta,\psi)=-\log\left(1-\frac{1-\cos\left[\frac{\pi}{2}\left(1-\bar{H}(t;\psi)^2\right)^{\eta}\right]}{1-\vartheta\cos\left[\frac{\pi}{2}\left(1-\bar{H}(t;\psi)^2\right)^{\eta}\right]}\right). \tag{2.13}$$

2.2. Series Expansion of the PDF

The PDF of the MOCTL-G family can be expanded using a binomial series expansion and power series representation of trigonometric functions. The binomial expansion:

$$(1-b)^{-m} = \sum_{i=0}^{\infty} \frac{\Gamma(m+i)}{\Gamma(m) i!} b^i, \quad \text{for } |b| < 1, m > 0, \tag{2.14}$$

is applied to the denominator of the PDF, giving:

$$\left[1 - \vartheta \cos\left(\frac{\pi}{2}\left(1 - \bar{H}(t;\psi)^2\right)^{\eta}\right)\right]^{-2} = \sum_{i=0}^{\infty} (i+1)\vartheta^i \left[\cos\left(\frac{\pi}{2}\left(1 - \bar{H}(t;\psi)^2\right)^{\eta}\right)\right]^i. \tag{2.15}$$

Using the Taylor series expansions of the trigonometric functions:

$$\cos z = \sum_{j=0}^{\infty} \frac{(-1)^j z^{2j}}{(2j)!}, \tag{2.16}$$

$$\sin z = \sum_{j=0}^{\infty} \frac{(-1)^j z^{2j+1}}{(2j+1)!}, \tag{2.17}$$

and expanding the power series:

$$\left(\sum_{j=0}^{\infty} a_j x^j\right) = \sum_{j=0}^{\infty} c_j x^j, \tag{2.18}$$

where $c_0 = a_0^j, \quad c_m = \left[\frac{1}{m a_0}\right] \sum_{j=1}^{m} (jn - m + j) a_j c_{m-j}, \quad \text{for } m \geq 1.$

Applying these expansions to the MOCTL-G PDF, we obtain:

$$f(t) = \sum_{i=0}^{\infty}\sum_{n=0}^{\infty}\sum_{m=0}^{\infty} \frac{(-1)^{n+m}(i+1)\vartheta^i}{2n!(2m+1)!} \left(\frac{\pi}{2}\right)^{n+m} H(t;\psi)(1-H(t;\psi)) \times \left(1 - (1 - H(t;\psi))^2\right)^{(\eta-1)+2n\eta+\eta(2m+1)}. \tag{2.19}$$

The reduced form of the PDF is

$$f(t) = \pi\vartheta\eta \sum_{i,j,k,m,n=0}^{\infty} \bar{\gamma}_{ijkmn} \Upsilon_k(t), \tag{2.20}$$

where$\bar{\gamma}_{ijkmn} = \begin{pmatrix} 2\alpha(m+n+1)-1 \\ j \end{pmatrix} \begin{pmatrix} 2j+1 \\ k \end{pmatrix} \frac{(i+1)\bar{\theta}^i c_n (-1)^{m+n+j+k} \left(\frac{\pi}{2}\right)^{m+n}}{2n!(2m+1)!}$ and $\Upsilon_k(x;\tau) = h(x;\tau)[H(x;\tau)]^k.$

2.3. Quantile Function (QF)

The QF of MOCTL-G family $Q(u)$ is derived as:

$$Q(u) = H^{-1}\left\{1 - \left[1 - \left(\frac{\pi}{2} - \cos^{-1}\left(1 - \frac{u\vartheta}{1 - u\bar{\vartheta}}\right)\right)^{\frac{1}{\eta}}\right]^{\frac{1}{2}}\right\}. \tag{2.21}$$

This function allows for efficient simulation and generation of random samples from the MOCTL-G distribution.

2.4. Moments and Moment-Generating Function (MGF)

We formulate the moments and the MGF of the MOCTL-G distribution.

2.4.1. Moments

The r^{th} raw moment of the MOCTL-G family is given by:

$$\mu'_r = E\left[T^r\right] = \int_0^\infty t^r f(t)dt. \tag{2.22}$$

Substituting the expanded form of $f(t)$ from Eq. (2.19), we obtain:

$$\mu'_r = \pi\vartheta\eta \sum_{i,j,k,m,n=0=0}^{\infty} \gamma_{ijkmn} \int_0^\infty t^r \Upsilon_k(t)dt. \tag{2.23}$$

2.4.2. Moment-Generating Function

The MGF of the MOCTL-G family is expressed as:

$$M_Y(t) = E\left[e^{ty}\right] = \int_0^\infty e^{ty} f(y)dy. \tag{2.24}$$

Substituting the expanded form of $f(t)$ from Eq. (2.19), we obtain:

$$M_X(t) = \pi\vartheta\eta \sum_{i,j,k,m,n=0}^{\infty} \gamma_{ijkmn} \int_0^\infty e^{t^* t} \Upsilon_k(t)dt. \tag{2.25}$$

2.5. Rényi Entropy

Rényi's entropy of the MOCTL-G distribution is express as:

$$I_r = \frac{1}{1-\eta} \log \int_0^\infty f(y)^\eta dy, \quad \eta > 0, \eta \neq 1. \tag{2.26}$$

Substituting the expanded form of $f(t)$ from Eq. (2.19), we obtain:

$$I_r = \frac{1}{1-\eta}\log\left(\pi^\eta\vartheta^\eta\eta^\eta\sum_{i,j,k,m,n=0}^{\infty}\gamma_{ijkmn}\int_0^\infty \Upsilon_k(t)^\eta dt\right). \tag{2.27}$$

2.6. Order Statistics

The PDF of the i^{th} order statistic in a random sample of size m drawn from the MOCTL-G distribution is define as:

$$f_{i,m}(t) = \frac{m!}{(i-1)!(m-i)!}f(t)F(t)^{i-1}(1-F(t))^{m-i}. \tag{2.28}$$

Expanding the CDF of MOCTL-G, we obtain:

$$f_{i,n}(t) = \frac{f(t)}{B(i,n-i+1)}\sum_{j=0}^{n-i}\binom{n-i}{j}(-1)^j\left[\frac{1-\cos\left(\frac{\pi}{2}(1-\bar{H}(t;\psi)^2)^\eta\right)}{1-\vartheta\cos\left(\frac{\pi}{2}(1-\bar{H}(t;\psi)^2)^\eta\right)}\right]^{i+j-1}. \tag{2.29}$$

2.7. Parameter Estimation

Parameter estimation for the MOCTL-G distribution is carried out using the method of MLE. Suppose $t_1, t_2, \ldots, t_n$ represents a random sample drawn from the MOCTL-G distribution. The corresponding likelihood function can be expressed as:

$$L(\eta,\vartheta,\psi) = \prod_{i=1}^{n} f(t_i). \tag{2.30}$$

Taking the natural logarithm, we obtain the log-likelihood function:

$$\begin{aligned}\ell = n\log\pi + n\log\vartheta + n\log\eta + \sum_{i=1}^{n}\log h(t_i;\psi) + \sum_{i=1}^{n}\log(1-H(t_i;\psi)) + (\eta-1)\sum_{i=1}^{n}\log(1-(1-H(t_i;\psi))^2)\\ + \sum_{i=1}^{n}\log\sin\left(\frac{\pi}{2}(1-(1-H(t_i;\psi))^2)^\eta\right) - 2\sum_{i=1}^{n}\log\left(1-\vartheta\cos\left(\frac{\pi}{2}(1-(1-H(t_i;\psi))^2)^\eta\right)\right).\end{aligned} \tag{2.31}$$

2.7.1. Score Functions

The score function components, defined as $U(\vartheta) = \left(\frac{\delta\ell}{\delta\eta}, \frac{\delta\ell}{\delta\vartheta}, \frac{\delta\ell}{\delta\psi}\right)^T$, are derived as follows:

$$\begin{aligned}\frac{\delta\ell}{\delta\eta} = \frac{n}{\eta} + \sum_{i=1}^{n}\log(1-(1-H(t_i;\psi))^2) + \frac{\pi}{2}\sum_{i=1}^{n}(1-H(t_i;\psi))\log(1-(1-H(t_i;\psi))^2)\cot\left(\frac{\pi}{2}(1-(1-H(t_i;\psi))^2)^\eta\right)\\ + \vartheta\pi\sum_{i=1}^{n}(1-H(t_i;\psi))\log(1-(1-H(t_i;\psi))^2)\tan\left(\frac{\pi}{2}(1-(1-H(t_i;\psi))^2)^\eta\right).\end{aligned} \tag{2.32}$$

$$\frac{\delta \ell}{\delta \vartheta} = \frac{n}{\vartheta} - \sum_{i=1}^{n} \log \cos\left(\frac{\pi}{2}(1-(1-H(t_i;\psi))^2)^{\eta}\right). \tag{2.33}$$

$$\begin{aligned}\frac{\delta \ell}{\delta \psi} = &\sum_{i=1}^{n} \frac{h'(t_i;\psi)}{h(t_i;\psi)} - \sum_{i=1}^{n} \frac{H'(t_i;\psi)}{1-H(t_i;\psi)} + 2(\eta-1)\sum_{i=1}^{n} \frac{H'(t_i;\psi)}{1-(1-H(t_i;\psi))^2} \\ &+ \eta\pi \sum_{i=1}^{n} H'(t_i;\psi)(1-H(t_i;\psi))(1-(1-H(t_i;\psi))^2)^{\eta-1} \cot\left(\frac{\pi}{2}(1-(1-H(t_i;\psi))^2)^{\eta}\right).\end{aligned} \tag{2.34}$$

3. Some Sub Models of the MOCTL-G Family

Here, we present two sub models of the MOCTL family by using two well-known classical distributions: the Weibull and the Gompertz distributions. The PDFs, CDFs, HRF, and SF for each case are analyzed and visualized to explore the flexibility of the proposed models.

3.1. Marshall-Olkin Cosine Topp-Leone Weibull (MOCTLW) Distribution

By using the Weibull distribution as the baseline model, we define the MOCTLW distribution with the following CDF:

$$F(t;\eta,\vartheta,\gamma,\omega) = \frac{1-\cos\left[\frac{\pi}{2}\left(1-e^{-2\gamma x^{\omega}}\right)^{\eta}\right]}{1-\overline{\vartheta}\cos\left[\frac{\pi}{2}\left(1-e^{-2\gamma x^{\omega}}\right)^{\eta}\right]}. \tag{3.1}$$

The corresponding probability density function (PDF) is:

$$f(t;\eta,\vartheta,\gamma,\omega) = \frac{\pi\eta\vartheta\gamma\omega t^{\omega-1}e^{-\gamma t^{\omega}}e^{-\gamma t^{\omega}}\left(1-e^{-2\gamma t^{\omega}}\right)^{\eta-1}}{\left(1-\overline{\vartheta}\cos\left[\frac{\pi}{2}\left(1-e^{-2\gamma t^{\omega}}\right)^{\eta}\right]\right)^2} \times \sin\left[\frac{\pi}{2}\left(1-e^{-2\gamma t^{\omega}}\right)^{\eta}\right]. \tag{3.2}$$

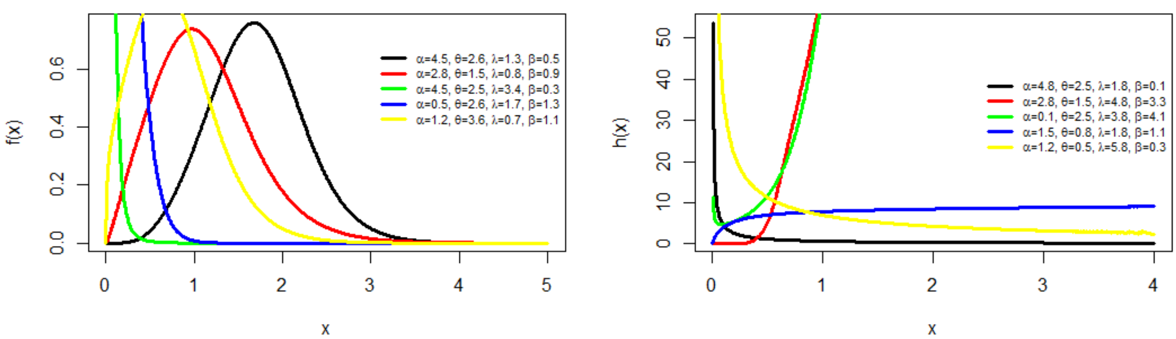

Figure 1. PDF and Hazard Function of the MOCTLW Distribution

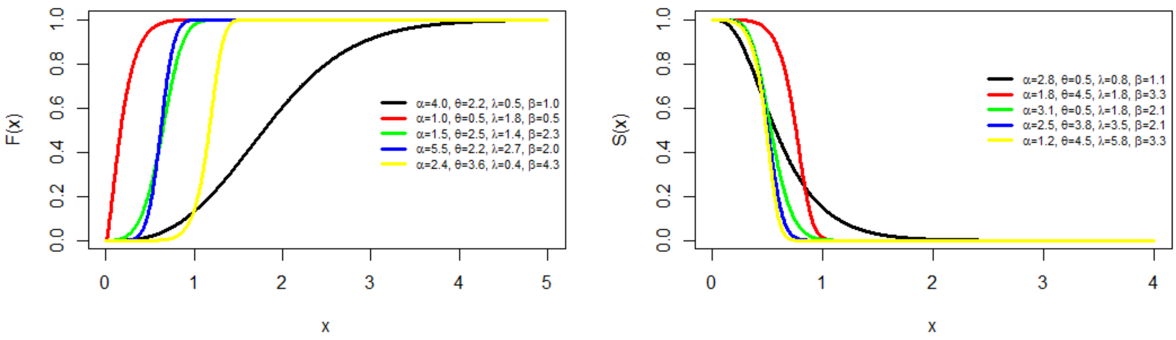

Figure 2. CDF and Survival Function of the MOCTLW Distribution

Figure 1 displays the plots of the PDF and HRF for various parameter settings. The PDF demonstrates a range of shapes, including right-skewed and reversed J-forms, while the HRF reveals diverse patterns such as increasing, unimodal, and nearly constant behaviors. Additionally, Figure 2 presents the CDF and SF plots, further illustrating the flexibility of the MOCTL-G distribution under different parameter configurations.

3.2. Marshall-Olkin Cosine Topp-Leone Gompertz (MOCTLG) Distribution

Using the Gompertz distribution as the baseline, we define the MOCTLG distribution with the corresponding density and distribution functions.

$$F(t;\eta,\vartheta,\lambda,\alpha) = \frac{1-\cos\left[\frac{\pi}{2}\left(1-e^{-\frac{\alpha}{\lambda}\left(e^{\lambda t}-1\right)}\right)^{\eta}\right]}{1-\bar{\vartheta}\cos\left[\frac{\pi}{2}\left(1-e^{-\frac{\alpha}{\lambda}\left(e^{\lambda t}-1\right)}\right)^{\eta}\right]}, \tag{3.3}$$

and

$$f(t;\eta,\vartheta,\alpha,\lambda) = \frac{\pi\eta\vartheta\alpha e^{\lambda t}e^{-\frac{\alpha}{\lambda}\left(e^{\lambda t}-1\right)}\left(1-e^{-\frac{\alpha}{\lambda}\left(e^{\lambda t}-1\right)}\right)^{\eta-1}}{2\left(1-\bar{\vartheta}\cos\left[\frac{\pi}{2}\left(1-e^{-\frac{\alpha}{\lambda}\left(e^{\lambda t}-1\right)}\right)^{\eta}\right]\right)^{2}} \times \sin\left[\frac{\pi}{2}\left(1-e^{-\frac{\alpha}{\lambda}\left(e^{\lambda t}-1\right)}\right)^{\eta}\right]. \tag{3.4}$$

The PDF and HRF plots for the MOCTL-G distribution, as shown in Fig. 3, reveal flexible behaviors across different parameter values. The density function is right-skewed and nearly symmetric, while the HRF exhibits varying trends of increase and decrease. Fig. 4 presents the CDF and SF plots.

4. Survival Regression Model

This section introduces the Log Marshall-Olkin Cosine Topp-Leone Weibull Regression Model (LMCTLW-RM) as an extension of the MOCTLW distribution for survival analysis.

Using the following transformation $Y = \log T$, the log-transformed LMCTLW density function is:

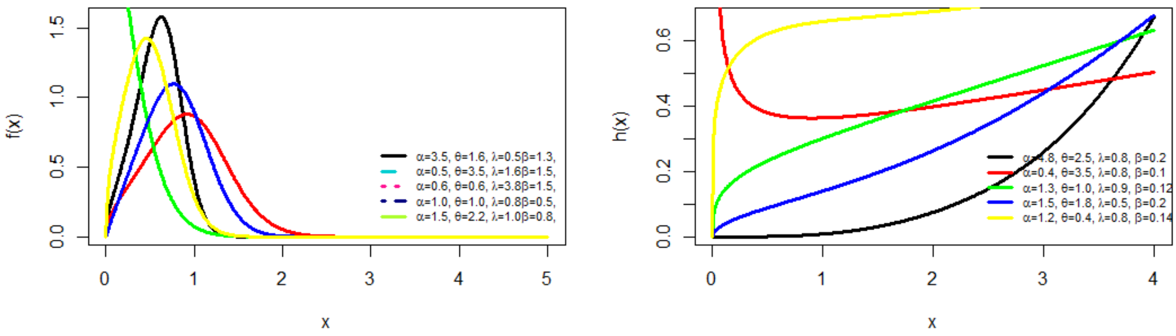

Figure 3. PDF and Hazard Function of the MOCTLG Distribution

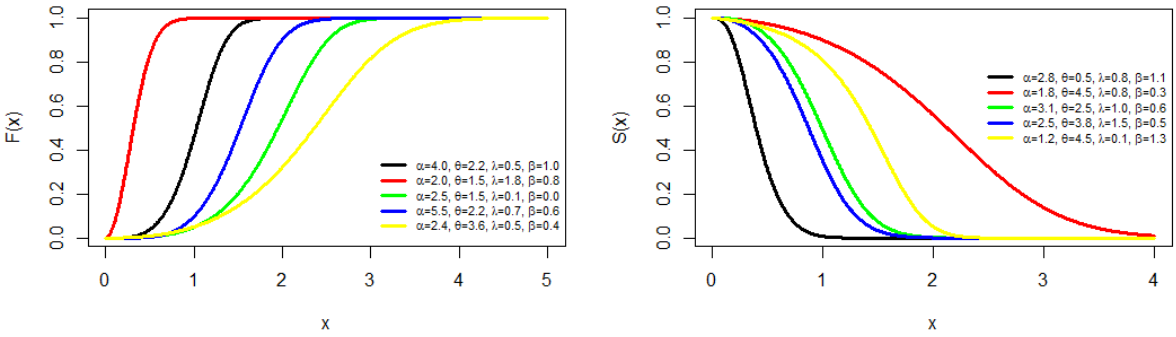

Figure 4. CDF and Survival Function of the MOCTLG Distribution

$$f(y;\eta,\vartheta,\mu,\sigma)=\frac{\frac{\vartheta\pi\eta}{2\sigma}e^{\frac{y-\mu}{\sigma}-e^{\frac{y-\mu}{\sigma}}}\left(1-e^{-e^{\frac{y-\mu}{\sigma}}}\right)^{\eta-1}}{\left(1-\overline{\vartheta}\cos\left[\frac{\pi}{2}\left(1-e^{-e^{\frac{y-\mu}{\sigma}}}\right)^{\eta}\right]\right)^{2}}\times\sin\left[\frac{\pi}{2}\left(1-e^{-e^{\frac{y-\mu}{\sigma}}}\right)^{\eta}\right]. \tag{4.1}$$

The survival function of Y is:

$$S(y;\eta,\vartheta,\mu,\sigma)=1-\frac{1-\cos\left[\frac{\pi}{2}\left(1-e^{-e^{\frac{y-\mu}{\sigma}}}\right)^{\eta}\right]}{1-\overline{\vartheta}\cos\left[\frac{\pi}{2}\left(1-e^{-e^{\frac{y-\mu}{\sigma}}}\right)^{\eta}\right]}. \tag{4.2}$$

Let $z=\frac{y-\mu}{\sigma}$. We define the MOCTLW location-scale regression model as:

$$y_i=\mathbf{t}_i^T\boldsymbol{\omega}+\sigma z_i,\quad i=1,2,\ldots,n. \tag{4.3}$$

where: - $\mathbf{t}_i^T$ is the vector of explanatory variables, - z_i follows the LMCTLW distribution, - $\boldsymbol{\omega}$ is the vector of regression coefficients.

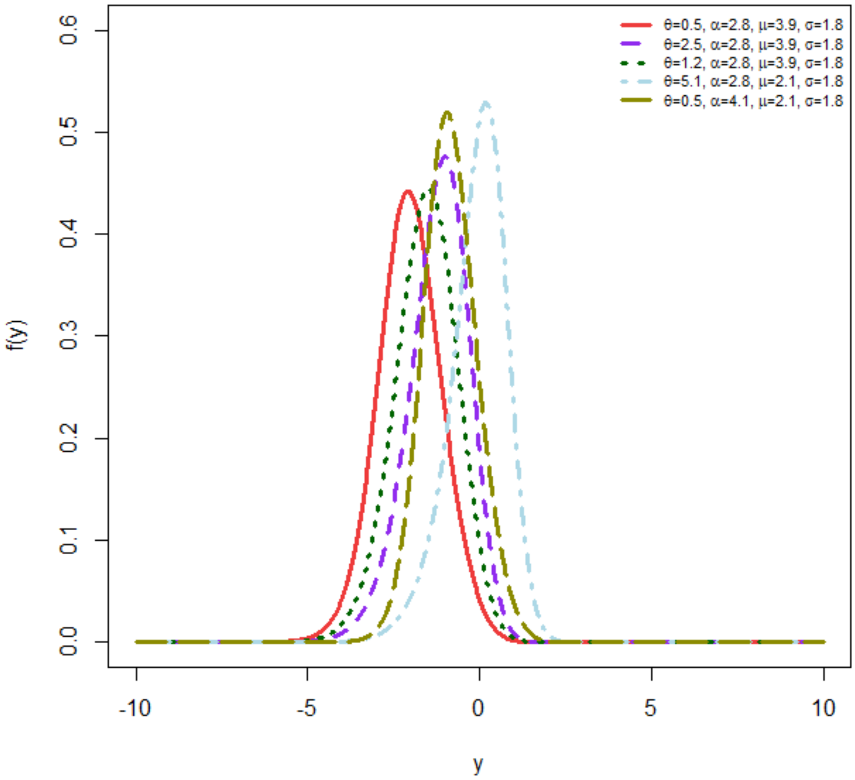

Figure 5. PDF plot of the LMCTLW Distribution

4.1. Parameter Estimation

For a sample of n observations $\{(y_i, \mathbf{t}_i)\}$, the likelihood function under right-censoring is:

$$\ell(\boldsymbol{\omega}) = \sum_{i \in T} \ell_1(\boldsymbol{\omega}) + \sum_{i \in C} \ell_2(\boldsymbol{\omega}), \tag{4.4}$$

where T and C represent uncensored and censored cases, respectively.

4.2. Residual Analysis

To assess model adequacy, Cox-Snell residuals are computed as:

$$e_i = -\log\left[S\left(y_i|t_i\right)\right]. \tag{4.5}$$

For the LMCTLW regression model, this simplifies to:

$$e_i = -\log\left\{1 - \frac{1 - \cos\left[\frac{\pi}{2}\left(1 - e^{-e^{\frac{y_i - \hat{\omega}^T \hat{t}_i}{\sigma}}}\right)^{\eta}\right]}{1 - \overline{\vartheta}\cos\left[\frac{\pi}{2}\left(1 - e^{-e^{\frac{y_i - \hat{\omega}^T \hat{t}_i}{\sigma}}}\right)^{\eta}\right]}\right\}. \tag{4.6}$$

If the model is well-fitted, these residuals should follow an exponential distribution.

5. Simulation Study

To assess the performance of the maximum likelihood estimators (MLEs) for the MOCTL-Weibull (MOCTLW) distribution, we conduct an extensive Monte Carlo simulation study with 1,000 iterations across varying sample sizes. Data are generated using the quantile function (QF) of the MOCTLW distribution based on specified true parameter values. The BFGS optimization algorithm was implemented in R with box constraints to ensure parameter validity, with complete reproducibility ensured through supplementary R code. We evaluate the accuracy and efficiency of the MLEs using bias and mean squared error (MSE). The simulation results presented in Table 1 reveal consistent patterns across all parameters. As expected from asymptotic theory, both bias and mean squared error (MSE) decrease monotonically with increasing sample size, confirming the consistency of the MLEs.

6. Empirical Applications of the MOCTLW Distribution

This section demonstrates the practical utility of the Marshall-Olkin Cosine Topp-Leone Weibull (MOCTLW) distribution through comprehensive empirical analyses. We evaluate its performance against four established competing models:

6.1. Goodness-of-Fit Framework

We employ a rigorous evaluation framework consisting of:

6.1.1. Information Criteria

- Akaike Information Criterion (AIC): $-2\ell + 2k$
- Bayesian Information Criterion (BIC): $-2\ell + k\log n$
- Consistent AIC (CAIC): $-2\ell + 2kn/(n-k-1)$

where ℓ is the log-likelihood, k is the number of parameters, and n is the sample size.

6.1.2. Nonparametric Tests

- Cramér-von Mises (W): $\frac{1}{12n} + \sum_{i=1}^{n}\left(F_n(x_i) - \frac{2i-1}{2n}\right)^2$
- Anderson-Darling (A^2): $-n - \frac{1}{n}\sum_{i=1}^{n}(2i-1)[\ln F_n(x_i) + \ln(1-F_n(x_{n+1-i}))]$
- Kolmogorov-Smirnov (D): $\sup_x |F_n(x) - F(x)|$

For all measures, lower values indicate superior model fit. The comprehensive comparison across these metrics provides robust evidence of the MOCTLW distribution's enhanced flexibility and applicability in real-world scenarios.

6.2. Application to Kevlar Fatigue Fracture Dataset

The first case study examines fatigue life measurements for Kevlar 373/epoxy composite materials under constant stress conditions. The dataset, originally studied by [43], records the time-to-failure

Table 1. Simulation results for the MOCTLW distribution ($\vartheta = 0.3$, $\eta = 3.0$, $\gamma = 2.5$, $\omega = 1.6$)

Sample Size	Parameter	MLE Estimate	Bias	MSE
n=25	ϑ	0.4400	0.1400	0.4320
	η	2.9937	-0.0063	0.6853
	γ	2.8367	0.3367	0.9116
	ω	1.7076	0.1076	0.3581
n=50	ϑ	0.3965	0.0965	0.3176
	η	3.0516	0.0516	0.5581
	γ	2.6963	0.1963	0.5173
	ω	1.6381	0.0381	0.2507
n=75	ϑ	0.3773	0.0773	0.2673
	η	3.0981	0.0981	0.4775
	γ	2.6376	0.1376	0.5131
	ω	1.6041	0.0041	0.1950
n=150	ϑ	0.3596	0.0596	0.2047
	η	3.0995	0.0995	0.3154
	γ	2.5732	0.0732	0.3424
	ω	1.5816	-0.0184	0.1417
n=250	ϑ	0.3474	0.0474	0.1628
	η	3.0848	0.0848	0.2672
	γ	2.5569	0.0569	0.2845
	ω	1.5811	-0.0189	0.1160
n=500	ϑ	0.3340	0.0340	0.1242
	η	3.0685	0.0685	0.1941
	γ	2.5364	0.0364	0.2173
	ω	1.5800	-0.0200	0.0873
n=1000	ϑ	0.3247	0.0247	0.0941
	η	3.0517	0.0517	0.1534
	γ	2.5303	0.0303	0.1712
	ω	1.5829	-0.0171	0.0680

Table 2. Competing models for comparative analysis

Model	Description
CTLW	Cosine Topp-Leone Weibull [31]
TrCTLW	Transmuted Cosine Topp-Leone Weibull [40]
ExCTLW	Exponentiated Cosine Topp-Leone Weibull [41]
TLW	Topp-Leone Weibull [42]

(in hours) for 76 specimens subjected to a constant 90% stress level. These complete failure times make this dataset particularly valuable for lifetime modeling applications in materials science. The dataset values are as follows: ”0.0251, 0.0886, 0.0891, 0.2501, 0.3113, 0.3451, 0.4763, 0.5650, 0.5671, 0.6566, 0.6748, 0.6751, 0.6753, 0.7696, 0.8375, 0.8391, 0.8425, 0.8645, 0.8851, 0.9113, 0.9120, 0.9836, 1.0483, 1.0596, 1.0773, 1.1733, 1.2570, 1.2766, 1.2985, 1.3211, 1.3503, 1.3551, 1.4595, 1.4880, 1.5728, 1.5733, 1.7083, 1.7263, 1.7460, 1.7630, 1.7746, 1.8275, 1.8375, 1.8503, 1.8808, 1.8878, 1.8881, 1.9316, 1.9558, 2.0048, 2.0408, 2.0903, 2.1093, 2.1330, 2.2100, 2.2460, 2.2878, 2.3203, 2.3470, 2.3513, 2.4951, 2.5260, 2.9911, 3.0256, 3.2678, 3.4045, 3.4846, 3.7433, 3.7455, 3.9143, 4.8073, 5.4005, 5.4435, 5.5295, 6.5541, 9.0960”.

The comparative model evaluation, presented in Table 3, demonstrates the superior performance of the MOCTLW distribution across all information criteria. Specifically, the MOCTLW yields the lowest values for the Akaike Information Criterion (AIC), Bayesian Information Criterion (BIC), and related metrics, indicating its better fit relative to competing models. To further validate these findings, we conducted complementary nonparametric goodness-of-fit tests, with detailed results summarized in Table 4. The MOCTLW distribution consistently outperforms the alternative models, as reflected in its lower Anderson-Darling and Cramér–von Mises statistics, along with a more favorable Kolmogorov–Smirnov (K–S) test outcome.

Table 3. Model parameter estimates and information criteria for Kevlar Fracture Dataset

Model	ϑ	η	γ	ω	AIC	CAIC	BIC	Rank
ExCTLW	0.3391	2.0164	0.2534	1.1363	251.733	261.0557	252.2964	4
TrCTLW	-0.7165	0.6467	0.3565	1.0082	250.7038	260.0267	251.2672	2
MOCTLW	39.7946	1.8274	1.9392	0.4438	**248.3684**	**257.6913**	**248.9317**	**1**
CTLW	-	0.6733	1.1829	0.2300	251.6326	261.0468	251.9095	3
TLW	-	1.4356	1.1042	0.2881	251.7463	261.0602	252.3067	5

Table 4. Goodness-of-fit test results for dataset one

Model	$-\ell\ell$	A^* (p-value)	CVM (p-value)	KS (p-value)
ExCTLW	121.8615	0.6836 (0.0924)	0.1158 (0.0671)	0.0954 (0.4249)
TrCTLW	121.3519	0.5534 (0.1487)	0.0949 (0.1296)	0.0944 (0.4781)
MOCTLW	**120.1842**	**0.4139 (0.1900)**	**0.0582 (0.1800)**	**0.0904 (0.5220)**
CTLW	122.8163	0.6804 (0.0727)	0.1154 (0.0676)	0.0987 (0.4617)
TLW	122.8632	0.6846 (0.0710)	0.1161 (0.0663)	0.0990 (0.4187)

Figure 6 provides a graphical representation of the fitted density curves. The MOCTLW model (black curve) closely follows the histogram bars, indicating its superior fit compared to alternative models.

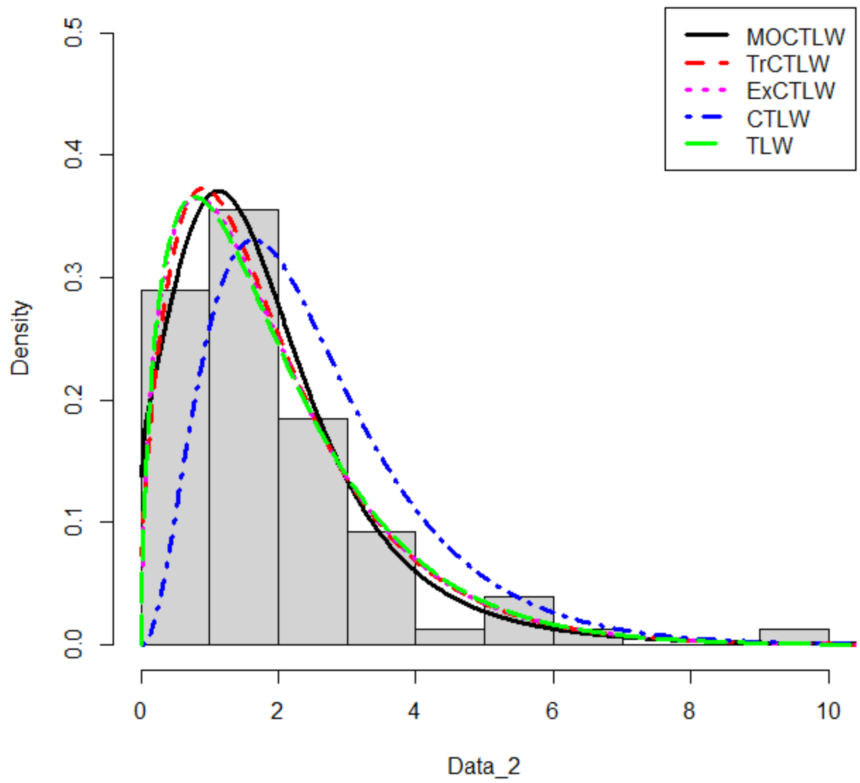

Figure 6. Density plot of the fitted models using dataset one

6.3. Application to Acute Lymphocytic Leukaemia in children Datasets

The second dataset was compiled in 1981 by the Pediatric Oncology Group (POG) as part of a multi-center prospective study on standard-risk acute lymphocytic leukemia (ALinC) in children. The data was previously used by [44] and is illustrated as: 1.3 1 1.2 0.9 1.1 0.8 0.5 1 0.7 0.5 1.7 1.1 0.8 0.5 1.2 0.8 1.1 0.9 1.2 0.9 0.8 0.6 0.3 0.8 0.6 0.4 1.1 1.1 0.2 0.8 0.5 1.1 0.1 0.8 1.7 1 0.8 1 0.8 1 0.2 0.8 0.4 1 0.2 0.8 1.4 0.8 0.5 1.1 0.9 1.3 0.9 0.4 1.4 0.9 0.5 1.7 0.9 0.8 0.8 1.2 0.9 0.8 0.5 1 0.6 0.1 0.2 0.5 0.1 0.1 0.9 0.6 0.9 0.6 1.2 1.5 1.1 1.4 1.2 1.7 1.4 1 0.7 0.4 0.9 0.7 0.8 0.7 0.4 0.9 0.6 0.4 1.2 2 0.7 0.5 0.9 0.5 0.9 0.7 0.9 0.7 0.4 1 0.7 0.9 0.7 0.5 1.3 0.9 0.8 1 0.7 0.7 0.6 0.8 1.1 0.9 0.9 0.8 0.8 0.7 0.7 0.4 0.5 0.4 0.9 0.9 0.7 1 1 0.7 1.3 1 1.1 1.1 0.9 1.1 0.8 1 0.7 1.6 0.8 0.6 0.8 0.6 1.2 0.9 0.6 0.8 1 0.5 0.8 1 1.1 0.8 0.8 0.5 1.1 0.8 0.9 1.1 0.8 1.2 1.1 1.2 1.1 1.2 0.2 0.5 0.7 0.2 0.5 0.6 0.1 0.4 0.6 0.2 0.5 1.1 0.8 0.6 1.1 0.9 0.6 0.3 0.9 0.8 0.8 0.6 0.4 1.2 1.3 1 0.6 1.2 0.9 1.2 0.9 0.5 0.8 1 0.7 0.9 1 0.1 0.2 0.1 0.1 1.1 1 1.1 0.7 1.1 0.7 1.8 1.2 0.9 1.7 1.2 1.3 1.2 0.9 0.7 0.7 1.2 1 0.9 1.6 0.8 0.8 1.1 1.1 0.8 0.6 1 0.8 1.1 0.8 0.5 1.5 1.1 0.8 0.6 1.1 0.8 1.1 0.8 1.5 1.1 0.8 0.4 1 0.8 1.4 0.9 0.9 1 0.9 1.3 0.8 1 0.5 1 0.7 0.5 1.4 1.2 0.9 1.1 0.9 1.1 1 0.9 1.2 0.9 1.2 0.9 0.5 0.9 0.7 0.3 1 0.6 1 0.9 1 1.1 0.8 0.5 1.1 0.8 1.2 0.8 0.5 1.5 1.5 1

0.8 1 0.5 1.7 0.3 0.6 0.6 0.4 0.5 0.5 0.7 0.4 0.5 0.8 0.5 1.3 0.9 1.3 0.9 0.5 1.2 0.9 1.1 0.9 0.5 0.7 0.5 1.1 1.1 0.5 0.8 0.6 1.2 0.8 0.4 1.3 0.8 0.5 1.2 0.7 0.5 0.9 1.3 0.8 1.2 0.9.

Table 5. The results of MLE estimates and values of information criteria for ALinC dataset

Model	θ	α	λ	β	AIC	CAIC	BIC	Rank
ExCTLW	0.2665	1.4278	0.4094	3.2022	232.4144	247.8002	232.5317	3
TrCTLW	-0.6682	0.3507	0.5331	2.8618	229.1552	244.5410	229.2725	2
MOCTLW	25.7302	0.5705	1.9606	1.2969	221.2374	236.6232	221.3547	1
CTLW	-	0.3830	3.3258	0.3829	233.5574	248.9670	233.6275	5
TLW	-	0.8090	3.0689	0.4740	232.519	248.0852	232.5891	4

Table 5 displays the parameter estimates and GOF metrics for the competing distributions analyzed using the ALinC dataset. The evaluation is based on criteria such as the AIC, BIC, and CAIC, where lower values indicate a better fit. The analysis reveals that the MOCTLW distribution provides the best fit, outperforming the other competing models.

The study incorporated additional discrimination measures, including the A^*, CVM, and KS tests, to compare the proposed distribution with alternative models. Corresponding p-values were also computed. Table 6 presents a summary of these statistical measures. The best-fitting probability model is typically identified as the one with the lowest KS, A^*, and CVM values, alongside the highest p-values. A review of the results confirms that the MOCTLW model outperforms the competing models, making it a suitable choice for analyzing the ALinC dataset.

Table 6. The results of the GOF test for ALinC dataset

Model	$-\ell\ell$	A^* (p-value)	CVM (p-value)	KS (p-value)
ExCTLW	112.2072	2.6690 (<0.0001)	0.4568 (<0.0001)	0.0879 (0.0095)
TrCTLW	110.5776	2.4367 (0.0173)	0.4274 (<0.0001)	0.0829 (0.0173)
MOCTLW	106.6187	2.2409 (0.0513)	0.4176 (<0.0001)	0.0499 (0.0201)
CTLW	113.7787	2.9137 (<0.0001)	0.4974 (<0.0001)	0.0915 (0.0006)
TLW	113.1595	2.8034 (<0.0001)	0.4785 (<0.0001)	0.0902 (0.00072)

Figure 7 presents a histogram overlaid with fitted density plots for various probability distributions applied to the ALinC dataset. By examining the alignment between the fitted densities and the histogram bars, we can assess how well each distribution represents the data. A closer match suggests a more accurate fit. Notably, the MOCTLW distribution, depicted by the black curve, emerges as the best-fitting model for this dataset.

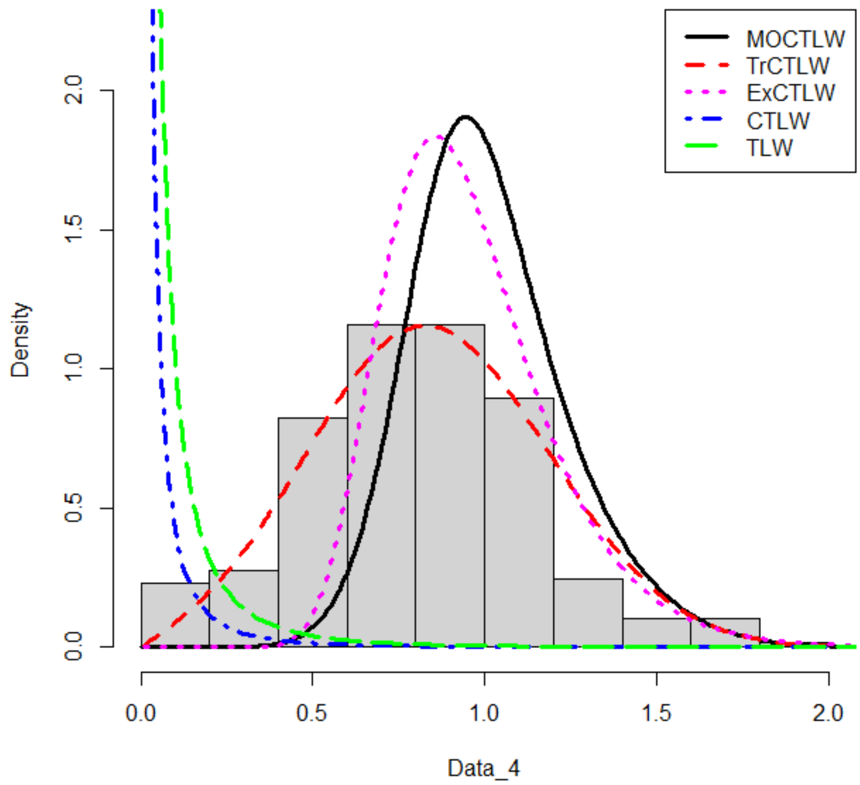

Figure 7. Curve of density of the proposed fitted model using ALinC dataset

6.4. Applications of Survival Regression Models for US COVID-19 data

The performance of the Log-Marshall-Olkin Cosine Topp-Leone Weibull (LMCTLW) and Log-Cosine Topp-Leone Weibull (LCTLW) regression models is assessed using the US COVID-19 dataset. This dataset, obtained from the WHO website, contains records of 425 patients admitted to US health facilities with COVID-19 between January and June 2022. Among these patients, 61.6% were censored, while 38.4% were uncensored. The response variable, denoted as y_i, represents the log of the observed survival time in days. The censoring indicator variable d is defined such that $d = 0$ corresponds to censored observations, while $d = 1$ denotes uncensored cases (patients who experienced the event which is death).

The definition of exposure variables:

- t_1: Age: ≤ 30 year (NO=0, YES=1)
- t_2: Age: $30 < Age \leq 60$ year (NO=0, YES=1)
- t_3: Age: > 60 year (NO=0, YES=1)
- t_4: Sex: male (NO=0, YES=1)
- t_5: Sex: female (NO=0, YES=1)
- t_6: Has acute respiratory distress syndrome (Positive=1, Negative=0)
- t_7: Has arrhythmia (NO=0, YES=1)

- t_8: Coughing (NO=0, YES=1)
- t_9: Has fever (NO=0, YES=1)
- t_{10}: Having difficulty breathing (NO=0, YES=1)
- t_{11}: Travel a lot (NO=0, YES=1)
- t_{12}: Has chronic disease (NO=0, YES=1)
- t_{13}: Has cardiovascular disease (NO=0, YES=1)
- t_{14}: Has Diabetes (Negative=0, Positive=1)
- t_{15}: Is hypertensive (Non-hypertensive=0, hypertensive=1)

The fitted regression model can be expressed as:

$$y_i = \beta_0 + \sum_{j=0}^{15} \beta_i t_{ij} + \sigma z_i, \qquad i = 1, 2, ..., 425. \tag{6.1}$$

The response variable is defined as $y_i = \log_e(t_i)$, representing the natural logarithm of the observed survival times in days, which follows either the LMCTLW or LCTLW distribution. The term z_i denotes the random error, whose density is given in Equation (6.1). The parameter $\sigma > 0$ is an unknown scale parameter, while $\boldsymbol{\beta} = (\beta_0, \beta_1, \ldots, \beta_{15})$ represents the set of unknown regression coefficients. Additionally, $\mathbf{t}^T = (\mathbf{t_0}, \mathbf{t_1}, \ldots, \mathbf{t_{15}})$ corresponds to the exposure variables.

The parameters of the regression models were estimated using the MLE method, implemented via the "mle2" function from the "bbmle" package in R. The performance of the fitted models was evaluated and compared using various statistical criteria. Table 7 presents the estimated parameters, their standard errors (SEs), corresponding p-values, and key goodness-of-fit metrics. Among the models considered, the log-Marshall-Olkin Cosine Topp-Leone Weibull (LMCTLW) regression model exhibits the lowest AIC and BIC values, indicating a superior fit compared to the log-Cosine Topp-Leone Weibull (LCTLW) model. These results suggest that the LMCTLW model is the most appropriate choice for modeling the given dataset.

The regression model parameters were estimated using the MLE approach, facilitated through the `mle2` function available in the `bbmle` package in R. To assess and compare the performance of the fitted models, several statistical measures were employed. Table 7 summarizes the estimated parameters along with their standard errors (SEs), associated p-values, and key GOF indicators. Among the models evaluated, the log-Marshall-Olkin Cosine Topp-Leone Weibull (LMCTLW) regression model yields the lowest values for the AIC and BIC, suggesting that it offers a better fit than the log-Cosine Topp-Leone Weibull (LCTLW) model. These findings support the LMCTLW model as the more suitable choice for analyzing the dataset.

In all fitted models, the coefficients for the explanatory variables-age below 30 years, age above 60 years, ARDS, arrhythmia, and travel history; were significant at the 5% level. The coefficients for age above 60 years, ARDS, and arrhythmia were negative, while the coefficient for travel history was positive. These findings indicate that the likelihood of survival decreases with increasing age. Furthermore, patients without ARDS, arrhythmia, and difficulty breathing tend to have longer survival times than those who present with these conditions.

Table 7. The estimates of the regression parameters and goodness-of-fit statistics for the COVID-19 dataset

Model	Parameters	Estimate	SE	P-value	Goodness-of-fit	Rank
	α	4.619674	7.9873	0.5630		
	θ	2.9366	3.6033	0.4150		
	σ	3.3178	1.9552	0.0897		
	β_0	-0.7818	2.7287	0.7744		
	β_1	1.9622	1.1859	0.0980		
	β_2	0.0430	0.8608	0.9601		
	β_3	-1.8872	0.8519	0.0267		
Log-LMCTLW	β_4	0.3204	1.3721	0.8153	AIC=773.969	1
	β_5	0.3977	1.3637	0.7705	BIC=846.907	
	β_6	-0.9321	0.2641	0.0004		
	β_7	-1.6239	0.5291	0.0021		
	β_8	-0.1543	0.4382	0.7246		
	β_9	0.0884	0.4382	0.8401		
	β_{10}	1.6164	0.3943	4.1e-05		
	β_{11}	1.0822	1.1653	0.3530		
	β_{12}	-0.9033	1.2034	0.4528		
	β_{13}	-1.7593	1.1850	0.1376		
	β_{14}	-1.3084	1.1649	0.2613		
	β_{15}	0.0403	0.7386	0.9564		
	α	1.5688	1.0851	0.1482		
	σ	2.0700	0.7397	0.0051		
	β_0	2.70474	0.6933	9.5e-05		
	β_1	2.5058	0.6912	0.0002		
	β_2	0.4272	0.2861	0.1354		
	β_3	-1.5284	0.2822	6.1e-08		
	β_4	-0.4335	0.3602	0.2288	AIC=775.313	2
Log-LCTLW	β_5	-0.3617	0.3609	0.3162	BIC=852.302	
	β_6	-0.9324	0.2684	0.0005		
	β_7	-1.5482	0.5487	0.0047		
	β_8	-0.1440	0.4408	0.7437		
	β_9	0.0776	0.4324	0.8575		
	β_{10}	1.6674	0.4204	7.3e-05		
	β_{11}	1.0569	1.1356	0.3520		
	β_{12}	-0.8675	1.1768	0.4610		
	β_{13}	-1.7132	1.1556	0.1382		
	β_{14}	-1.2663	1.1370	0.2653		
	β_{15}	0.0844	0.7679	0.9124		

6.4.1. Cox-Snell Residuals Analysis for COVID-19 Patients Data

Residual analysis is an essential step in validating survival regression models, as it helps evaluate the adequacy of the model fit by comparing observed survival probabilities with predicted values. In this study, we assess the goodness-of-fit for the LMCTLW and LCTLW regression models using Cox-Snell residuals (CSR). Figures 8 and 9 display the residual plots for both models, providing insights into their fit and any potential deviations from the expected behavior.

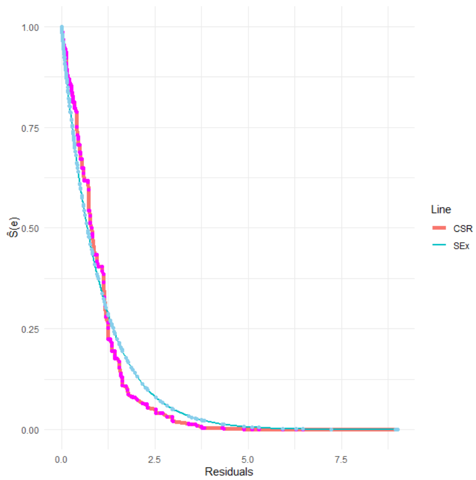

Figure 8. Cox-Snell Residuals Plot for COVID-19 Data using LMCTLW Model

For the LMCTLW model, the Kolmogorov-Smirnov one-sample test produces a test statistic of $D = 0.0947$, which is below the critical value of $D = 0.1065$ at the 5% significance level. This suggests that the (CSR) closely align with the standard exponential distribution, thereby confirming the adequacy of the LMCTLW model for inference.

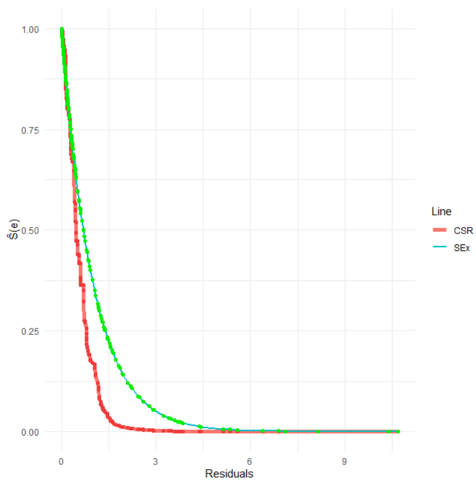

Figure 9. Cox-Snell Residuals Plot for COVID-19 Data using LCTLW Model

Using the Kolmogorov-Smirnov one-sample test, the test statistic for Figure 9 is $D = 0.2345$, which exceeds the critical value of $D = 0.1065$ at the 5% significance level. This suggests that the (CSR) for the LCTLW regression model do not follow the standard exponential distribution, meaning the model is not suitable for inference.

Figures 8 and 9 present the Cox-Snell residual plots for the LMCTLW and LCTLW regression models, respectively. The estimated standard exponential curve fits the theoretical survival curve more closely for the LMCTLW model than for the LCTLW model. While the Kolmogorov-Smirnov test statistic confirms that the LMCTLW model adequately fits the COVID-19 data, the LMCTLW regression model remains the most appropriate choice for inference.

7. Conclusion

This study introduces the Marshall-Olkin Cosine Topp-Leone (MOCTL-G) family of distributions, a flexible parametric model that enhances existing distribution families by incorporating additional shape parameters. We explore its fundamental characteristics, including moments, entropy, moment-generating functions, and order statistics. Furthermore, we develop survival regression models based on the MOCTL-G family to examine the relationships between survival time and exposure variables. A Monte Carlo simulation study demonstrates the reliability of the MLE for parameter estimation within the proposed distribution. The practical applicability of the MOCTL-G family is illustrated by fitting two real-life data. The MOCTLW distribution provides a better fit compared to some existing lifetime models. In the analysis of COVID-19 survival data, the Log-MOCTLW (LMCTLW) regression model outperforms the Log-CTLW (LCTLW) model according to goodness-of-fit criteria. Additionally, Cox-Snell residual analysis further validates the LMCTLW model as the most appropriate for inference. The findings suggest that the MOCTL-G family offers a robust framework for modeling survival data and can be applied to other real-world scenarios requiring flexible parametric distributions. Future research could expand on this work by exploring Bayesian estimation techniques, alternative parameter estimation methods, and applying the MOCTL-G family to a wider variety of survival datasets across fields such as medicine, engineering, and reliability studies.

Data Availability: The data that support the findings of this study are included in the manuscript.
Funding Statement This work was supported and funded by the Deanship of Scientific Research at Imam Mohammad Ibn Saud Islamic University (IMSIU) (grant number IMSIU-DDRSP2501).
Author contributions: All authors have accepted responsibility for the entire content of this manuscript and approved its submission.
Conflicts of interest: The authors declare that they have no conflicts of interest to report on the present study.
Acknowledgments This work was supported and funded by the Deanship of Scientific Research at Imam Mohammad Ibn Saud Islamic University (IMSIU) (grant number IMSIU-DDRSP2501).

References

1. Sarhadi, A., Burn, D. H., Concepcion Ausin, M., and Wiper, M. P. (2016). Time-varying nonstationary multivariate risk analysis using a dynamic Bayesian copula. Water Resources Research, 52(3), 2327–2349.
2. Ghitany, M. E., Al-Awadhi, F., and Alkhalfan, L. A. (2007). Marshall–Olkin extended Lomax distribution and its application to censored data. Communications in Statistics - Theory and Methods, 36(10), 1855–1866.

3. Gupta, R.D., Kundu, D. (1999). Generalized exponential distributions. *Australian and New Zealand Journal of Statistics*, 41(2), 173–188
4. Marshall, A.W., Olkin, I. (1997). A new method a parameter to a family for adding with to the exponential and application of distributions Weibull families. Biometrika, 84(3), 641–652.
5. Eugene, N., Lee, C., Famoye, F. (2002). Beta Normal Distribution and its Applications, Communications in Statistics - Theory and Methods, 31(4) 497–512.
6. Shaw, W. T., & Buckley, I. R. (2007). The alchemy of probability distributions: Beyond gram-charlier & cornish-fisher expansions, and skew-normal or kurtotic-normal distributions. Submitted, Feb, 7, 64.
7. Ahmad, Z., Elgarhy, M., Hamedani, G., & Butt, N. S. (2020). Odd generalized NH generated family of distributions with application to exponential model. *Pakistan Journal of Statistics and operation research*, 16(1), 53-71.
8. Alyami, S. A., Elbatal, I., Alotaibi, N., Almetwally, E. M., Okasha, H. M., & Elgarhy, M. (2022). Topp–Leone modified Weibull model: Theory and applications to medical and engineering data. Applied Sciences, 12(20), 10431.
9. Cordeiro, G.M., Castro, M. (2011). A new family of generalized distributions. Journal of statistical computation and simulation, 81(7), 883–898.
10. Zografos, K., Balakrishnan, N. (2009). On families of beta-and generalized gamma-generated distributions and associated inference. Statistical methodology, 6(4),344–362.
11. Tahir, M., Cordeiro, G.M., Alzaatreh, A., Mansoor, M., Zubair, M. (2016). The logistic-x family of distributions and its applications. Communications in statistics-Theory and methods, 45(24), 7326–7349.
12. Lee, C., Famoye, F., Alzaatreh, A.Y. (2013). Methods for generating families of uni-variate continuous distributions in the recent decades. Computational Statistics, 5(3), 219–238.
13. Cordeiro, G.M., Lemonte, A.J., Ortega, E.M. (2014). The marshall-olkin family of distributions: Mathematical properties and new models. Journal of Statistical Theory and Practice, 8, 343–366.
14. Nassar, M., Kumar, D., Dey, S., Cordeiro, G.M., Afify, A.Z. (2019). The marshall–olkin alpha power family of distributions with applications. Journal of Computational and Applied Mathematics, 351, 41–53.
15. Sandhya, E., & Prasanth, C. B. (2014). Marshall-Olkin Discrete Uniform Distribution. Journal of probability, 2014(1), 979312.
16. Yousof, H.M., Afify, A.Z., Nadarajah, S., Hamedani, G., Aryal, G.R. (2018). The marshall-olkin generalized-g family of distributions with applications. Statistica, 78(3), 273–295.
17. Khaleel, M. A., Oguntunde, P. E., Al Abbasi, J. N., Ibrahim, N. A., & AbuJarad, M. H. (2020). The Marshall-Olkin Topp Leone-G family of distributions: A family for generalizing probability models. Scientific African, 8, e00470.
18. Sherwani, R.A.K., Ashraf, S., Abbas, S., Aslam, M. (2023). Marshall olkin exponentiated dagum distribution: Properties and applications. Journal of Statistical Theory and Applications, 22(1), 70–97.

19. Chipepa, F., Moakofi, T., Oluyede, B. (2022). The marshall-olkin-odd power generalized weibull-g family of distributions with applications of covid-19 data. Journal of Probability and Statistical Science, 20(1), 1–20.

20. Rannona, K., Oluyede, B., Chipepa, F., Makubate, B. (2022). The marshall-olkin-type ii topp-leone-g family of distributions: Model, properties and applications. Journal of Probability and Statistical Science, 20(1), 127–149.

21. Naz, S., Tahir, M. H., Jamal, F., Elgarhy, M., Shafiq, S., Alsadat, N., & Nagarjuna, V. B. (2024). A new Marshall-Olkin generalized-k family of distributions with applications. Physica Scripta, 99(12), 125221.

22. Oluyede, B., Peter, P.O., Ndwapi, N. (2024). The exponentiated half-logistic-generalized marshall-olkin-g family of distributions with properties and applications. Thailand Statistician, 22(4), 779–802.

23. Abonongo, J., Mwaniki, I. J., & Aduda, J. A. (2024). Cosine Fréchet loss distribution: properties, actuarial measures and insurance applications. Computational Journal of Mathematical and Statistical Sciences, 3(1), 1-32.

24. Ameeq, M., Naz, S., Tahir, M., Muneeb Hassan, M., Jamal, F., Fatima, L., Shahzadi, R. (2024). A new marshall-olkin lomax distribution with application using failure and insurance data. Statistics, 58(2), 450–472.

25. Adepoju Akeem Ajibola, Isa Alhaji Modu, Bello Olalekan Akanji. Cosine Marshal-Olkin g family of Distribution. *Reliability: Theory & Applications*, 3(79), 408–422.

26. Al-Babtain, A.A., Elbatal, I., Chesneau, C., Elgarhy, M. (2020). Sine topp-leone-g family of distributions: Theory and applications. Open Physics, 18(1), 574–593.

27. Chesneau, C., Jamal, F.: The sine kumaraswamy-g family of distributions. *Journal of Mathematical Extension*, (2020) 15.

28. Benchiha, S., Sapkota, L.P., Al Mutairi, A., Kumar, V., Khashab, R.H., Gemeay, A.M., Elgarhy, M., Nassr, S.G. (2023). A new sine family of generalized distributions: Statistical inference with applications. Mathematical and Computational Applications, 28(4), 83.

29. Isa, A. M., Bashiru, S. O., Ali, B. A., Adepoju, A. A., & Itopa, I. I. (2022). Sine-exponential distribution: Its mathematical properties and application to real dataset. UMYU Scientifica, 1(1), 127-131.

30. Souza, L., O Júnior, W. R. D., Brito, C. C. R. D., Chesneau, C., Fernandes, R. L., & Ferreira, T. A. (2021). Tan-G class of trigonometric distributions and its applications. Cubo (Temuco), 23(1), 1-20.

31. Nanga, S., Nasiru, S., & Dioggban, J. (2023). Cosine Topp–Leone family of distributions: properties and regression. Research in Mathematics, 10(1), 2208935.

32. Alyami, S. A., Hassan, A. S., Elbatal, I., Alotaibi, N., Gemeay, A. M., & Elgarhy, M. (2024). Estimation methods based on ranked set sampling for the arctan uniform distribution with application. AIMS Mathematics, 9(4), 10304-10332.

33. Alotaibi, N., Al-Moisheer, A. S., Elbatal, I., Elgarhy, M., & Almetwally, E. M. (2024). Bayesian and Non-Bayesian Analysis for the Sine Generalized Linear Exponential Model under Progressively Censored Data. Computer Modeling in Engineering & Sciences, 140(3), 2795-2823.
34. Semary, H. E., Chesneau, C., Aldahlan, M. A., Elbatal, I., Elgarhy, M., Abdelwahab, M. M., & Almetwally, E. M. (2024). Univariate and bivariate extensions of the truncated inverted arctan power distribution with applications. Alexandria Engineering Journal, 100, 340-356.
35. Alyami, S. A., Elbatal, I., Alotaibi, N., Almetwally, E. M., & Elgarhy, M. (2022). Modeling to factor productivity of the United Kingdom food chain: Using a new lifetime-generated family of distributions. Sustainability, 14(14), 8942.
36. Muhammad, M., Bantan, R. A., Liu, L., Chesneau, C., Tahir, M. H., Jamal, F., & Elgarhy, M. (2021). A new extended cosine—G distributions for lifetime studies. Mathematics, 9(21), 2758.
37. Alzeley, O., Almetwally, E. M., Gemeay, A. M., Alshanbari, H. M., Hafez, E. H., & Abu-Moussa, M. H. (2021). Statistical Inference under Censored Data for the New Exponential-X Fréchet Distribution: Simulation and Application to Leukemia Data. Computational Intelligence and Neuroscience, 2021(1), 2167670.
38. Shrahili, M., Elbatal, I., Almutiry, W., & Elgarhy, M. (2021). Estimation of sine inverse exponential model under censored schemes. Journal of Mathematics, 2021(1), 7330385.
39. Chesneau, C., Bakouch, H. S., Hussain, T., & Para, B. A. (2021). The cosine geometric distribution with count data modeling. Journal of Applied Statistics, 48(1), 124-137.
40. Osi, A.A., Doguwa, S.I., Abubakar, Y., Zakari, Y., Abubakar, U.: Transmuted cosine topp-leone g family of distributions: properties and applications. *Journal of the Nigerian Society of Physical Sciences*, (2024) 6(4), 2049 `https://doi.org/10.46481/jnsps.2024.2049`
41. Osi, A. A., Doguwa, S. I., Abubakar, Y., Zakari, Y., & Abubakar, U. (2024). Development of Exponentiated Cosine Topp-Leone Generalized Family of Distributions and its Applications to Lifetime Data. UMYU Scientifica, 3(1), 157-167.
42. Al-Shomrani, A., Arif, O., Shawky, A., Hanif, S., & Shahbaz, M. Q. (2016). Topp-Leone Family of Distributions: Some Properties and Application. Pakistan Journal of Statistics and Operation Research, 443-451.
43. Andrews, D. F., & Herzberg, A. M. (2012). *Data: a collection of problems from many fields for the student and research worker*. Springer Science & Business Media.
44. Gieser, P. W., Chang, M. N., Rao, P. V., Shuster, J. J., & Pullen, J. (1998). Modelling cure rates using the Gompertz model with covariate information. Statistics in medicine, 17(8), 831-839.